Molecularly Imprinted Polymer Microspheres Containing Photoswitchable Spiropyran-Based Binding Sites

Tibor Renkecz,[‡] Günter Mistlberger,[‡] Marcin Pawlak,[‡] Viola Horváth,[†] and Eric Bakker*[,‡]

[‡]Department of Inorganic and Analytical Chemistry, University of Geneva, Quai E.-Ansermet 30, CH-1211, Geneva, Switzerland
[†]MTA-BME Research Group of Technical Analytical Chemistry, Hungarian Academy of Sciences—Budapest University of Technology and Economics, Szent Gellért tér 4., H-1111, Budapest, Hungary

S Supporting Information

ABSTRACT: A versatile approach for the preparation of photoswitchable molecularly imprinted polymers (MIPs) is proposed where the selective recognition and the photoresponsive function are assumed by two different monomers. As a proof of concept, MIP microspheres were synthesized by precipitation polymerization for recognizing terbutylazine, a triazine-type herbicide. Formation of the selective binding sites was based upon H-bonding interactions between the template and the functional monomer methacrylic acid, whereas a polymerizable spiropyran unit was incorporated into the polymer matrix to provide light-controllable characteristics. A trifunctional monomer, trimethylolpropane trimethacrylate, was used as a cross-linker. The imprinted particles exhibited considerable morphological differences compared to their nonimprinted counterparts as observed by scanning electron microscopy. The imprinting effect was confirmed by equilibrium rebinding studies. The photoresponsiveness of the polymer particles was visualized by fluorescence microscopy and further characterized by spectroscopy. The template binding behavior could be regulated by alternating UV and visible light illumination when analyte release and uptake was observed, respectively. Binding isotherms fitted by the Freundlich model revealed the photomodulation of the number of binding sites and their average affinity. This facile synthetic approach may give an attractive starting point to endow currently existing highly selective MIPs with photoswitchable properties, thereby extending the scope of spiropyran-based photoresponsive smart materials.

KEYWORDS: photoswitching, spiropyran, molecularly imprinted polymer, triazine, precipitation polymerization
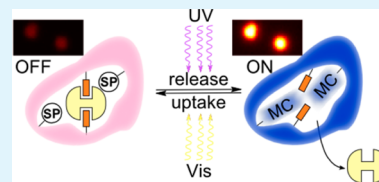
INTRODUCTION

The class of benzospiropyrans has attracted a rapidly increasing attention in the scientific community since their first description by Hirshberg in 1952.[1] Spiropyrans can adopt two different structures: a closed, rather nonpolar spiropyran (SP) form, and an open, highly polar merocyanine (MC) form (Figure 1). Upon photoinduced modulation the molecule can switch between its closed and open form. UV-irradiation transforms the molecule to MC, cleaving the C—O bond, whereas the ring-reclosure can be achieved by visible light or thermal stimuli. MC exists in two forms: a charge-separated, zwitterionic form appears in polar solvents, whereas in nonpolar solvents, the quinoidal form of the molecule is preferred.[2]

Because of the increased polarity of the open, merocyanine form it is stabilized in polar solvents, for instance in water or alcohols, and the rate of transformation back to the closed form is significantly decreased.[3,4]

The unique photoswitchable properties of spiropyrans can be utilized in many diverse fields including analytical chemistry, nanotechnology and materials science.[5−7] By incorporating spiropyran molecular units into solid supports, photoswitchable smart materials can be created with attractive properties as photocontrolled wettability, photoregulated swelling and shrinking, drug delivery and permeability. In sensor applications the desired system can be interrogated easily with a noninvasive stimulus (irradiation with light at a specific wavelength), providing a facile method for the regeneration of the recognizing surface. The binding interaction can also shift the absorbance spectra of the merocyanine offering a tool for quantitative analysis.[8]

The merocyanine form, which adsorbs in the visible spectral region, is able to bind metal ions,[8−12] amino acids,[13] DNA,[14]
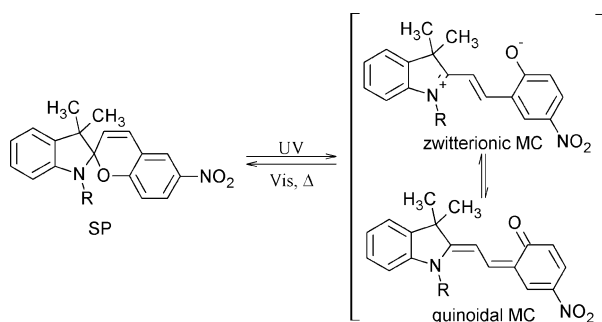

Figure 1. Photoisomerization of benzospiropyran.

H^{+}-ion[15] establishing an electrostatic interaction with the analyte of interest. The H^{+}-ion binding ability of MC in plasticized PVC membranes was recently exploited in our group for the development of reversible photodynamic sensors.[16−18]

A common problem with spiropyran based smart materials is the loss of reversibility induced by photodegradation, photo-bleaching, or photooxidation. This photofatigue occurs when the photoswitching cycle is repeated several times. Approaches can be found in the literature for reducing this phenomenon by the immobilization of spiropyran to a polymer matrix, either using spiropyran monomer derivatives or coupling the desired spiropyran to a polymer backbone.[15,19−21] It was reported that photofatigue can be decreased by using low-energy light sources, LEDs.[22]

Molecular imprinting can establish a predetermined selectivity toward a selected analyte (template) in a porous polymer matrix. MIPs are synthesized when the target molecule, acting as a template, is present in the prepolymeriza-tion solution and orients suitable functional monomers around itself by self-assembly.[23] The introduction of photochromic properties into molecularly imprinted polymers paves the way toward the selective, photocontrolled binding and release of the target compound. This could be exploited in affinity binding assays, sample cleanup and sensors.

Until now, relatively few papers have been published in the literature on molecularly imprinted polymers with photo-switching properties.[24−31] One publication from 1994 refers to molecular imprinting with a spiropyran acrylate monomer but there has been no follow-up of this work.[24] The other approaches use azobenzene type monomer units as the photocontrollable elements in the imprinted material that undergo cis−trans isomerization upon photomodulation.[25−31] Here, the azobenzene unit concurrently serves as the functional monomer. As azobenzene itself does not contain appropriate functional groups for the interaction with the template, many research groups have developed new functionalized azoben-zenes for this purpose using anilide,[25] carboxyl,[26] bisurea,[27] diaminopyridine,[28] sulfonic acid,[29] and pyridine[30,31] moieties. Most of the reported photocontrollable MIPs are bulk polymers and hydrogels that are often unsuited for the potential application since their processing requires cumber-some crushing, grinding and sieving steps. Zhang's group have introduced precipitation polymerization for the straightforward synthesis of photoswitchable azobenzene-based MIPs to directly create spherical microparticles.[30−33]

In this paper, we introduce a novel concept to the fabrication of photoswitchable MIP microspheres containing spiropyran as the photoactivatable unit. In contrast to current approaches, an additional functional monomer is also incorporated into the particles to enhance the selective recognition property of the polymer. The popular precipitation polymerization approach was chosen for preparing the microspheres due to its simplicity. Moreover, this one step-synthesis technique does not need any surfactants or stabilizers that could counteract the imprinting process.

Terbutylazine, a triazine type herbicide, was chosen as the model template because triazine imprinted polymers exhibit high imprinting efficiency and selectivity toward their template and its analogs due to the multiple interactions between the template and the functional monomer, methacrylic acid.[34−36] The obtained polymer exhibited a photoregulated binding behavior. The inherent photoswitching properties of the

particles were characterized by fluorescence microscopy and UV–vis spectroscopy. The selectivity between imprinted and nonimprinted polymer and the compound specificity were studied by equilibrium rebinding measurements. The Freund-lich isotherm model was used for detailed binding character-ization.

■ EXPERIMENTAL SECTION

Materials. Methacrylic acid (MAA, CAS no. 79−41−4, 99%), ethylene glycol dimethacrylate (EDMA, CAS no. 97−90−5, 99%), trimethylolpropane trimethacrylate (TRIM, CAS no. 3290−92−4, techn. gr.), 2,2′-azobisisobutyronitrile (AIBN, CAS no. 78−67−1, 98%), acetic acid (CAS no. 64−19−7, 99%), terbutylazine (CAS no. 5915−41−3, anal.std.), atrazine (CAS no. 1912−24−9, anal.std.), prometryn (CAS no. 7287−19−6, anal.std.), ametryn (CAS no. 834−12−8, anal.std.), and ketoprofen (CAS no. 22071−15−4, 98%) were purchased from Sigma-Aldrich (Seelze, Germany). HPLC grade acetonitrile (CAS no. 75−05−8, 99.95%) and toluene (CAS no. 108−88−3, 99.8%) were purchased from Biosolve Chimie (Val-kenswaard, The Netherlands). Methanol (CAS no. 67−56−1, 99.5%) was supplied by VWR International (Fontenay-sous-Bois, France).

1′-(2-Methacryloyloxyethyl)-3,3′-dimethyl-6-nitrospiro(2H-1ben-zopyran-2,2′-indoline) (spiropyran methacrylate, SPMA, CAS No. 25952−50−5) monomer was synthetized following previously reported procedures.[37] A detailed description is given in the Supporting Information. Water was purified with a Millipore Milli-Q Integral 3 system (Molsheim, France). MAA, EDMA and TRIM were purified before use by using a hydroquinone inhibitor remover column (Sigma-Aldrich, catalog no. 306312). The chemical structures of monomers, template, and related and nonrelated compounds can be seen in Figure 2.

Preparation of the Molecularly Imprinted Polymer Micro-spheres with Photoswitchable Spiropyran Unit. For the optimized polymer composition the template terbutylazine (9.2 mg, 0.04 mmol), MAA (14 mg, 0.16 mmol), spiropyran methacrylate (SPMA, 189 mg, 0.45 mmol), TRIM (132 mg, 0.39 mmol) and 3.4 mg (1 w/w% of monomers) AIBN initiator were weighted into a screw cap glass vial. The components were dissolved in 16.8 mL toluene (2
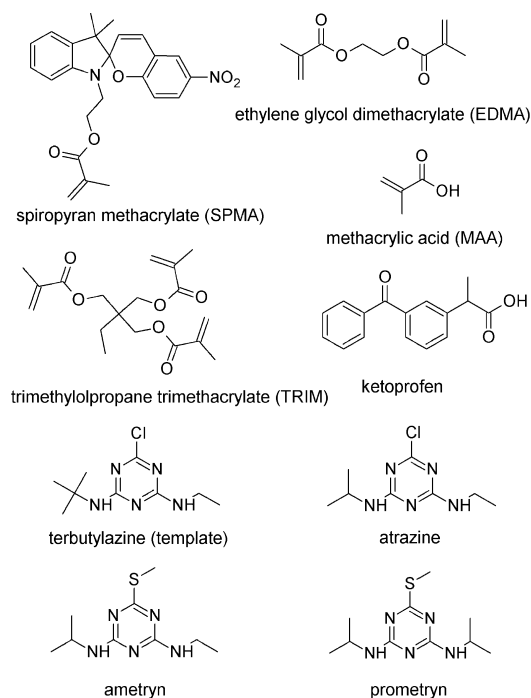

Figure 2. Chemical structure of monomers, template, analogous, and nonrelated compounds.

Table 1. Chemical Composition of the Studied MIPs and NIPs (the mol % of monomers is indicated in the brackets)

		template (mmol)	MAA (mmol)	SPMA (mmol)	EDMA (mmol)	TRIM (mmol)	AIBN (mg)	toluene (mL)
P1	MIP	0.08	0.32 [16%]		1.59 [84%]		3.4	16.8
	NIP							
P2	MIP	0.08	0.32 [16%]	0.10 [5%]	1.58 [79%]		3.8	19.2
	NIP							
P3	MIP	0.08	0.32 [16%]	0.30 [15%]	1.38 [69%]		4.3	21.3
	NIP							
P4	MIP	0.02	0.10 [5%]	0.30 [15%]	1.60 [80%]		4.5	22.5
	NIP							
P5	MIP	0.08	0.32 [16%]	0.45 [45%]	0.49 [39%]		3.1	15.7
	NIP							
P6	MIP	0.04	0.16 [16%]	0.45 [45%]		0.39 [39%]	3.4	16.8
	NIP							

w/v% monomer concentration). After deoxygenating the solution with nitrogen, the polymerization vessel was placed into a water bath thermostatted at 60 °C for 48 h in the dark. The precipitated polymer particles were collected by centrifugation and extensive batch-mode washing was performed by changing consecutively the washing solvent methanol-acetic acid (9:1) until no template was detected by HPLC. Finally, the polymers were washed with methanol, and left overnight for complete drying in a ventilated hood. Simultaneously, a nonimprinted polymer (NIP) was also prepared in the same manner as the MIP except that the template was omitted from the prepolymerization mixture. With the parallel evaluation of the binding properties of MIP and NIP one can acquire information about the efficiency of imprinting. Beside the above-mentioned optimal polymerization recipe, the detailed composition of the studied polymers (P1–P6) is summarized in Table 1.

Morphological Characterization. The morphological characterization of the polymer microparticles was carried out by scanning electron microscopy using a JEOL JSM-6510LV instrument. Samples were sputter coated with gold prior to analysis with a JEOL JFC-1200 Fine Coater. Particle size analysis was accomplished visually with the ImageJ software (National Institute of Health) selecting 200 individual particles from the SEM images of each sample.

Fluorescence Microscope Imaging. MIP polymer particles were incorporated into plasticized poly(vinyl chloride) thin film drop casted on glass slides. Imaging was carried out on a Nikon Eclipse Ti inverted microscope with a 20× Plan Fluar lens. For UV illumination the light of a xenon arc lamp (Lambda DG-4, Sutter Instrument Company) was filtered through a 365/20 nm bandpass filter (F49–365 ZET Laser Clean UP, Chroma) and reflected onto the sample using a 593 nm dichroic mirror. The fluorescence images were recorded using a Neo sCMOS camera (Andor). For imaging the deactivation process, a combination of a 413 nm long-pass filter (SR-FF02–409/LP-25, Semrock) and a 550 nm short-pass filter (FES0550, Thorlabs) was used for excitation. This combination allowed for sufficient light intensity for triggering the ring closure reaction while still enabling imaging of the fluorescence of the open form. The exposure times of the camera were adjusted to give the same maximum signal in both illumination modes.

Equilibrium Batch Rebinding Measurements. MIPs and nonimprinted polymers were weighted into polypropylene microtubes and the solution of the template (or analyte of interest) was pipetted on the particles in toluene or in acetonitrile. The phase ratio was set at 60, i.e., 60 μL solvent/mg polymer was applied in the experiments. The samples were shaken on a Fisher Vortex Genie 2 until equilibrium was reached without any light manipulation. The samples were centrifuged on a Hermle Z 100 M microcentrifuge to separate the particles. The supernatant was evaporated under gentle air stream in case of toluene and then reconstituted in eluent or diluted to eluent composition when using acetonitrile.

The concentration of the unbound analyte (c_e) was determined with HPLC. The HPLC system (JASCO, Japan) was operated with a Phenomenex Luna C-18, 4.6 × 125 mm, 5 μm column with a mobile

phase at a flow rate of 1 mL min^{-1}. The detector wavelength was set at 230 nm for the detection of triazines and at 260 nm for ketoprofen, the injection volume was 20 μL.

Mobile phase composition was 60–40% v/v acetonitrile–water mixture for terbutylazine, ametryn, and prometryn. It was modified as follows: for atrazine 50–50% v/v acetonitrile–water mixture, for ketoprofen 60–40% v/v acetonitrile–water mixture modified with 0.1% v/v acetic acid, and for the simultaneous separation of all five analytes 32–68% v/v acetonitrile–water mixture modified with 0.1% v/v acetic acid. All equilibrium batch rebinding measurements were done in triplicates.

From the equilibrium concentration the bound concentration of analyte can be calculated according to the following equation

$$q_e = \frac{(c_0 - c_e)V}{m} \tag{1}$$

where c_o and c_e are the initial and equilibrium concentration (mol L^{-1}) of the analyte, respectively. V is the volume of solution (L), m is the mass of the dry polymer (kg), and q_e is the adsorbed concentration expressed in (mol kg^{-1}). From q_e, one can calculate the distribution coefficient, D (L kg^{-1}):

$$D = \frac{q_e}{c_e} \tag{2}$$

Photocontrolled Binding and Release Study. A sequence of samples were incubated until equilibrium under identical conditions as mentioned in the previous section. The sampling was first carried out without UV light manipulation. After that, a set of samples were UV irradiated with a Herolab NU-4 UV Hand lamp (4 W, 365 nm) for 10 and 15 min, in toluene and acetonitrile, respectively and were analyzed.

For repetitive photomodulated binding cycles the samples were reincubated under visible white light until equilibrium was reached. A second UV irradiation in the same manner as before was applied. A third cycle with visible light was performed, converting the spiropyran units to their closed state. Sampling was performed after each step to gain information about changes in the binding capacity induced by the light manipulation.

Safety Consideration. Eye protective glasses should be worn during UV light manipulation of the samples.

■ RESULTS AND DISCUSSION

Preparation of Photoswitchable Terbutylazine Imprinted Microparticles. We put here forward a new strategy for the preparation of photoswitchable MIPs where a comonomer, methacrylic acid is mainly responsible for the selective recognition of the template while photochromic spiropyran monomers ensure the photocontrolled template binding and release. Photoisomerization induces structural changes in SPMA and drastic changes in the conformation of

8539

dx.doi.org/10.1021/am401958e | ACS Appl. Mater. Interfaces 2013, 5, 8537–8545

the polymer network, thereby also changing the spatial arrangement of the binding sites and expelling the template.

Precipitation polymerization was chosen as a straightforward and beneficial route for the synthesis of spherical MIP particles. This type of polymerization is often carried out either in acetonitrile or in a mixture of acetonitrile and toluene in order to ensure a satisfactory solubilization of the growing polymer chains.[38] Toluene is a good pore forming agent that endows the polymer matrix with a well-developed pore structure and high specific surface area, therefore increases the binding capacity of the sorbent.[39]

In this study, toluene was chosen as polymerization medium because triazine imprinted polymers have already been prepared with high imprinting efficiency in toluene by bulk[34−36] and precipitation polymerization.[40] Moreover, spiropyrans are known to exhibit faster photoswitching kinetics in apolar solvents.[4] The polymer synthesis was carried out thermally because UV initiation could have induced the ring-opening and also the photobleaching of the monomer. At elevated temperatures in polar aqueous solvents the SP molecule may open up because of the H-bonded stabilization of the merocyanine form.[41] For this reason, the use of the apolar toluene solvent is advantageous in a thermal polymerization approach.

In addition, methacrylic acid was chosen as an established functional comonomer responsible for the creation of selective recognition sites by interaction with the triazine molecule through multipoint H-bonding.[42] The required relative amounts of spiropyran and MAA as well as the quantity and type of cross-linker were explored by preparing polymers with different composition and testing their template binding ability in equilibrium batch-rebinding assays. The measurements were carried out in toluene, i.e., in the polymerization solvent where MIPs are expected to exhibit the highest specific binding.[43] In all these studies, the template concentration was 100 μM. Distribution coefficients (D) were calculated as a useful interpretation tool of results derived from the batch-binding experiments.[44]

Figure 3 presents the calculated distribution coefficients of the different polymers (P1−P6) both for imprinted and their
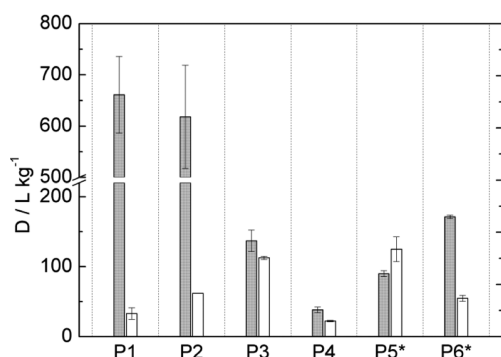

Figure 3. Distribution coefficients of the studied MIPs (gray) and NIPs (white) in 100 μM terbutylazine in toluene (asterisk indicates polymers with photoresponsive binding behavior).

nonimprinted counterparts. A detailed description of the different polymer compositions is given in Table 1. In parallel, all the polymers were tested for their photochromic properties to find whether illumination with UV light brings about a measurable release of the template. A polymer without

spiropyran was prepared for comparison using 16 mol % MAA and 84 mol % EDMA cross-linker (P1). Subsequently, 5 mol % SPMA and 16 mol % MAA were incorporated into the polymers at the expense of EDMA (P2). The original polymer composition gives high imprinting efficiency considering the much higher D value for the MIP (660 ± 75 L kg^{-1}) than that of the NIP (32 ± 8.2 L kg^{-1}). When spiropyran monomer was introduced into the polymer matrix (P2), a slight decrease in the distribution coefficient could be observed but the binding behavior was still quite similar to the initial composition. However, there was no measurable template release upon photoswitching. A further increase of the SPMA content to 15 mol % (P3) at the expense of the cross-linker (69 mol %), keeping the MAA content at 16 mol %, still could not trigger UV initiated template release. In another approach the high cross-linking level was kept at 80 mol % and SPMA was applied in excess compared to the functional monomer MAA (P4). However, the concentration of the spiropyran units in the polymer matrix still proved to be insufficient for the template release. Furthermore, a decrease in the distribution coefficients and imprinting efficiency was observed because of the inadequate amount of the comonomer MAA.

These findings suggested that a drastically increased SPMA content is required for light modulated template release, along with a high MAA content in order to retain sufficient binding capacity and selectivity. Accordingly, 45 mol % spiropyran monomer was used with 39 mol % EDMA cross-linker and 16 mol % functional monomer (P5). Photoresponsive release and binding behavior was now observed but no selectivity between MIP and the NIP was achieved. This was attributed to the reduced level of cross-linking, which is required to conserve the imprinted binding cavities during polymerization.

It has been reported that the trifunctional cross-linking monomer TRIM is superior to the commonly used bifunctional EDMA when used in lower cross-linking ratios.[45] It can provide a higher load capacity and the amount of functional monomer can safely exceed the amount of cross-linker without loss of performance. Therefore, a polymer with the above-mentioned molar composition was synthesized substituting EDMA with TRIM (P6). From Figure 3, it is clear that this MIP provided a distinct imprinting effect. It also exhibited UV-induced photocontrolled template binding behavior (for experimental results, see Photoregulated Template Uptake and Release Studies section). In the subsequent experiments, this polymer composition was characterized with different techniques.

Morphological Characterization. The morphology of the polymer microparticles with the optimal composition (P6) was investigated by scanning electron microscopy (SEM), see Figure 4. The imprinted particles exhibited regular spherical shape with a narrow size distribution (mean diameter 1.70 ± 0.2 μm), whereas the nonimprinted ones were irregular and smaller with a broad size distribution. This trend was observed also with MAA/EDMA particles without spiropyran functionality (see Figure S1 in the Supporting Information) which clearly indicates that the template influences the polymer formation. This suggests that the template−monomer complex changes the solubility of the growing polymer chains, thereby altering the polymer morphology. Typically, acetonitrile is used as solvent for the precipitation polymerization of methacrylate based MIPs resulting in regular, spherical microparticles. Acetonitrile with a solubility parameter (δ) of 24.6 MPa$^{0.5}$ is more polar than EDMA or TRIM (δ = 18.2 MPa$^{0.5}$)[40] and acts as a poor solvent of the forming methacrylate oligomers. This
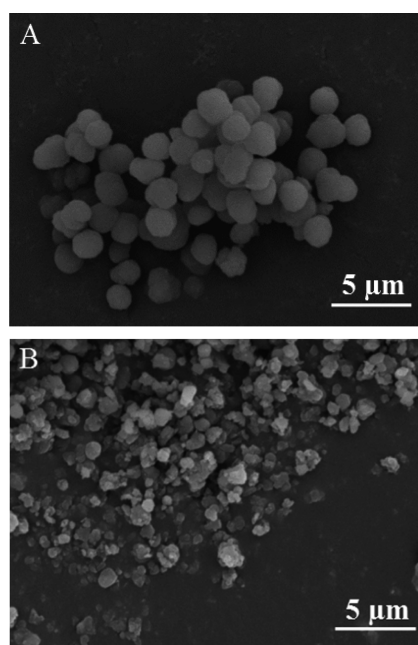
Figure 4. SEM images of molecularly (A) imprinted and (B) nonimprinted polymer microparticles containing spiropyran units.

results in an early phase separation during polymerization when the formed polymer nuclei precipitate. They then grow to larger polymer particles by capturing the residual soluble oligomers and monomers from the polymerization solution. Toluene (δ = 18.6 MPa$^{0.5}$)[38] is a better solvent of the methacrylate oligomers and phase separation is delayed. This allows for more nuclei to be formed gradually, resulting in smaller, irregular, aggregated particles when the template is absent. In the presence of the template the template-functional monomer complexes incorporated into the methacrylate oligomers shift the polarity of the chains toward the more polar range increasing the difference between the solubility parameter of toluene and the forming polymer network. This again leads to early phase separation, precipitation of the growing polymer chains and the formation of spherical microparticles.

Photoisomerization Properties of the MIP Microspheres. The photoactivatable properties of the MIP micro-

spheres were characterized and visualized by fluorescence microscopy. The polymer particles were immobilized into plasticized poly(vinyl chloride) on a glass slide. Figure 5 presents screenshots of a movie where the particles can be observed in their different photoswitched states. The first image in Figure 5 shows the fluorescence intensity of the incorporated open, merocyanine units in the particles after UV light irradiation. Subsequently, the fluorescence is continuously decreasing when exposed to visible light as observed in Figure 5-2−4. The reversibility of the photoswitching was confirmed with several alternating UV and Vis cycles and illustrated in Figure 5-5 and -6, respectively.

For the full movie showing 10 such cycles, see the Supporting Information. For the same experiment, the fluorescence intensity change with different light manipulation was analyzed by line profiles across two MIP particles in order to follow the activation and deactivation of single particles. The evolution of fluorescence after UV illumination exhibits faster kinetics compared to the reversed process. Fluorescence intensity data of the alternating activation−deactivation cycles as a function of time give information about the repeatability of the photoswitching on these particles. A ~34% decrease in the intensity could be observed after ten consecutive cycles which can be attributed to photobleaching triggered by the light source of the fluorescence microscope (Figure 6). In addition,
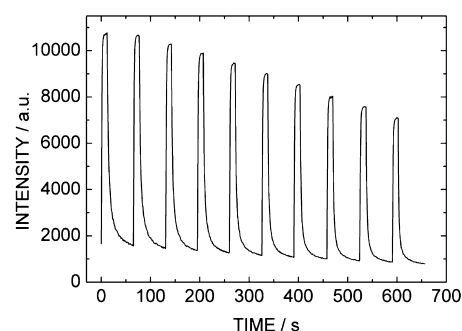

Figure 6. Photoswitching cycles of spiropyran containing MIP microspheres by fluorescence microscopy (UV λ_{irr}= 365/20 nm, time = 10 s, power = 0.4 W cm^{-2}; Vis λ_{irr} = 413−550 nm, time = 50 s, power = 8 W cm^{-2}).
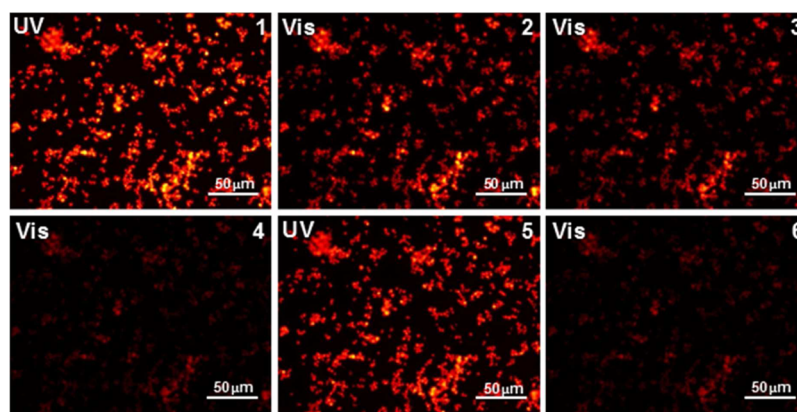

Figure 5. Fluorescence microscopy screenshots from a movie demonstrating the reversible photoswitching property of the MIP microparticles, Image 1, 5: 10 s UV (λ_{irr} = 365/20 nm, power = 0.4 W cm^{-2}); Image 2, 3, 4, 6: 2, 7, 55, 45 s visible light illumination (λ_{irr} = 413−550 nm, power = 8 W cm^{-2}), respectively.

the photoswitchable properties of the synthesized microparticles and the SPMA monomer were investigated by UV–vis spectroscopy in cuvette experiments. The discussion of these results can be found in the Supporting Information.

Binding Properties of the Photoswitchable MIP Microspheres. The binding kinetics of the spiropyran containing microparticles in 100 μM of terbutylazine was evaluated without UV light manipulation. The measured equilibrium time of ~90 min suggests fast template binding kinetics. Equilibrium batch rebinding measurements were carried out in a range of 10–3000 μM initial concentration of the template using a phase ratio of 60.

Batch sorption tests were evaluated in the form of adsorption isotherms, as it allows for a reliable characterization of MIPs.[46] The Freundlich model was applied to fit the adsorption isotherms before and after photomodulation and to gain information about the binding sites. This continuous distribution model has been widely used for MIPs since it can give an adequate approximation of the broad unimodal distribution compared to discrete binding models and the binding site heterogeneity can be quantified.[47] This model is a power function of the equilibrium concentration, and the bound amount of analyte in the polymer phase can be calculated with

$$B = aF^m \tag{3}$$

where B is the concentration of analyte in the polymer phase in units of (μmol g^{-1}), F is the equilibrium concentration in the solution phase in μM, a is the preexponential factor (μmol g^{-1} (μM^{-m})), and m is the heterogeneity index (unitless). From the binding parameters, a and m, one can calculate physical characteristics. The heterogeneity index, m can have a value between 0 and 1 where 1 corresponds to an entirely homogeneous binding. The method proposed by Rampey et al. was used to calculate the affinity distribution, number of binding sites, average weighted affinity from the binding isotherms (see tee Supporting Information for details).[47] The binding isotherms fitted with the Freundlich model for the imprinted and nonimprinted polymers are shown in Figure 7. The calculated binding parameters can be found in Table 2. The additional binding capacity created by the template results in a difference of 17.2 μmol g^{-1} between MIP and NIP comparing the respective values at the highest measured equilibrium concentration level of MIP (2109 μM).
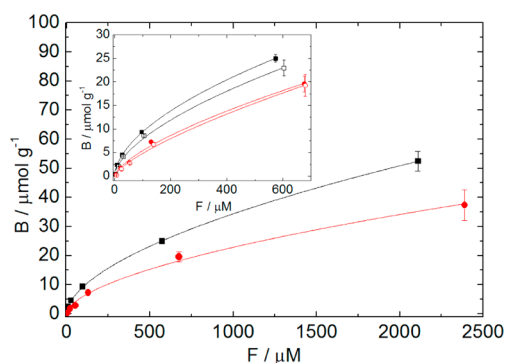

Figure 7. Binding isotherms of terbutylazine imprinted (black square) and nonimprinted polymers (red circle) in toluene, inset: initial part of the isotherms before UV (solid symbol) and after UV irradiation (open symbol, λ_{irr}= 365 nm, time = 10 min, power = 4 W).

Table 2. Freundlich Fitting Parameters and Calculated Values of Terbutylazine Imprinted and Nonimprinted Polymers with and without UV Light Manipulation

	MIP		NIP	
	before UV	after UV	before UV	after UV
a ((μmol g^{-1}) (μM)$^{-m}$)	0.69	0.48	0.42	0.29
m	0.57	0.60	0.58	0.64
r^2	0.9998	0.9995	0.9940	0.9970
$N_{Kmin–Kmax}$ (μmol g^{-1})	35.0	31.1	24.5	23.3
$K_{Kmin–Kmax}$ (L mmol^{-1})	12.6	7.66	7.22	5.65
K range (L mmol^{-1})	0.47–524	0.46–226	0.42–190	0.43–148

The irradiation time was optimized to achieve a maximum release of the previously bound analyte and to allow for the measurement of the binding isotherms after photomodulation. MIP microspheres were equilibrated with 10 μM terbutylazine in toluene and subsequently illuminated with UV light. Samples were taken from the supernatant at different time intervals and their triazine concentration was determined. The percentage of unbound analyte was calculated for each point and plotted against the UV exposure time. The results are shown in Figure S5 in the Supporting Information. Since the ring-opening kinetics is faster in more apolar solvents, less illumination time was necessary to achieve the new equilibrium in toluene. In toluene, the amount of the unbound template increased by 26% within 10 min and the remaining analyte was bound in the polymer matrix. In acetonitrile complete release of the template could be observed within 15 min. We have to point out, however, that the template binding is much weaker in acetonitrile compared to toluene which is attributable to the polar nature of this solvent.[35,36]

As it can be seen in Table 2, both the number of binding sites ($N_{Kmin-Kmax}$) and the average affinity constants ($K_{Kmin-Kmax}$) are higher in the imprinted polymer compared to the nonimprinted one. The value of m for the MIP indicates slightly more heterogeneous binding sites. This higher deviation from the homogeneous surface is probably the consequence of the imprinting whereby selective binding sites are also formed together with the nonselective ones. UV irradiation reduces the amount of binding sites ($N_{Kmin-Kmax}$) both on the MIP and the NIP. However, this effect is more pronounced on the imprinted polymer therefore the MIP can be considered more responsive to light illumination. Upon UV light impact also the binding affinity was reduced on both polymers and it was again more significantly affected in the imprinted polymer. One can conclude that photoswitching induces an important binding property change in the studied polymer system.

The cross-selectivity of the photoswitchable molecularly imprinted polymer was assessed with template analogs and a nonrelated compound both in individual and in mixed solutions of the analytes. Batch sorption experiments were carried out with three similar triazine derivatives, atrazine, ametryn and prometryn as well as a structurally different molecule, ketoprofen which has similar hydrophobicity (log P = 2.81) as the template (log P = 2.98).[40]

First, 50 μM toluene solutions of the individual analytes were applied in the batch sorption test in a phase ratio of 60. The calculated distribution coefficients are presented in Figure 8A. The highest binding on the MIP takes place with terbutylazine.
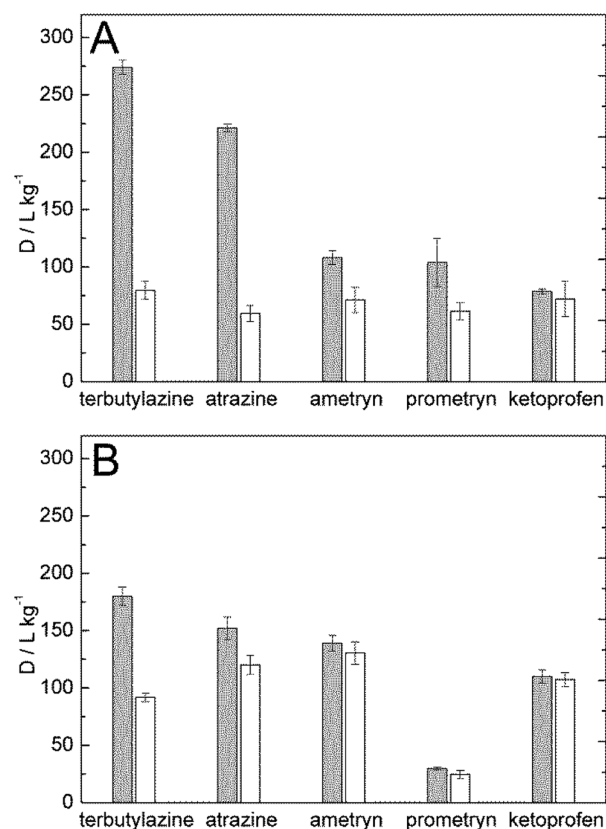
8542

dx.doi.org/10.1021/am401958e | *ACS Appl. Mater. Interfaces* 2013, 5, 8537–8545

Figure 8. Cross-selectivity study of spiropyran-containing MIPs (gray) and NIPs (white) in (A) individual analyte solution and (B) mixed solution.

The structurally similar analog atrazine shows very similar binding to the MIP. Ametryn and prometryn possess less structural resemblance to the template (the chlorine atom is changed to a thiomethyl group), which results in a significant decrease in their distribution coefficient. This arises from steric hindrance and a reduced access to the specific binding sites. The nonrelated compound ketoprofen does not show any selective binding since its distribution coefficients on the MIP and the NIP are the same. The triazine analogs also show very similar binding on the NIP. Ketoprofen binds to both polymers with nonspecific interactions, as well as the triazine analogs to the NIP. As the number of nonspecific binding sites is proportional to the surface area of the polymers we can presume that the imprinted and the nonimprinted polymers have very similar specific surface area. This indicates that the difference in binding of triazine analogs to the MIP and the NIP can be attributed to the selective sites and not to a difference in the surface area of these polymers.

Additionally, the selectivity study was carried out with a mixture of all analytes (50 μM each component). As it can be seen in Figure 8B, the selectivity order shows the same trend toward the template and its analogs on the MIP as observed in the individual solution tests albeit the binding is reduced due to the competitive adsorption of the molecules. The binding of prometryn (the most hydrophobic analyte in the study) is significantly suppressed because in toluene the retention mechanism is driven by normal-phase behavior, i.e., the more polar molecules are preferentially bound to the polymer. The adsorption of ketoprofen is slightly enhanced in the competitive conditions which might be attributed to synergistic effects

where the analytes assist the binding of the other compounds for instance by forming H-bonding between each other.

Photoregulated Template Uptake and Release Studies. The template and its analog prometryn were subjected to repeated photocontrolled binding-release cycles in toluene solutions at a concentration of 10 μM. The reversible operation of the photocontrolled binding sites was tested with alternating UV and visible light illumination. Figure 9 presents the photoresponsive binding behavior of the imprinted and nonimprinted polymers.
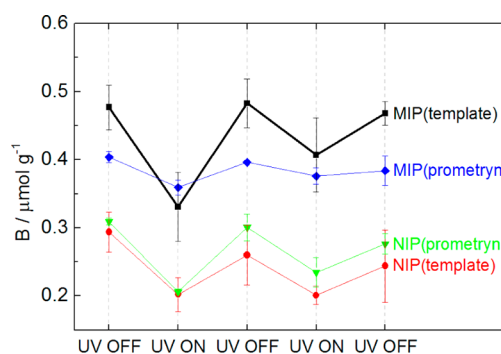

Figure 9. Binding behavior of the template terbutylazine (MIP, black square; NIP, red circle) and prometryn (MIP, blue diamond; NIP, green triangle) on imprinted and nonimprinted polymers performing repeated photoswitching cycles in 10 μM toluene solutions of the analyte (UV: λ_{irr} = 365 nm, time = 10 min, power = 4 W).

In the first step before UV light irradiation, the binding sites exist as they were formed during the polymerization, showing a high fidelity toward the template. When the UV light is turned on the spiropyran to merocyanine transformation results in a steric rearrangement of the polymer chains and the conformational change of the binding cavity induces a partial release of the bound molecules. The most significant release is achieved with the template molecule, corresponding to 30% reduction in the binding capacity. The efficiency of release probably correlates with the number of occupied binding sites in the vicinity of the spiropyran molecules. When visible light irradiation is used, rebinding takes place and the initially bound amount of template is regained. A subsequent UV manipulation resulted in the expulsion of a smaller amount of template. This signals a partial reduction of the photoresponsive binding sites, i.e., a fraction of the previously photoadjustable binding sites is not able to release the analyte again. This may be due to a diminution of the switchable spiropyran units, which was also observed in the photocyclic spectroscopic study and was attributed to the photobleaching of the molecules, possible merocyanine aggregations or merocyanine-polymer subgroup interactions. In case of prometryn the photoswitching ability is also detected but to a much smaller extent.

The presence of selective binding sites in the imprinted polymer is apparent since the binding capacity in every light manipulated step is higher compared to the nonimprinted counterpart. In the control polymer, the presence of photoswitchable binding sites is also detectable because in this polymer the photoswitchable spiropyran unit regulates the nonspecific binding.

CONCLUSIONS

In this paper, we demonstrated the preparation and characterization of photoswitchable molecularly imprinted polymer microspheres based on a novel strategy. Instead of using only one photochromic functional monomer, the well-established and widely used methacrylic acid took its role to form the selective binding sites and a spiropyran-based monomer was responsible for the photomodulation of the imprinted cavities.

The separation of the two different functions offers a possibly generic method to synthesize photocontrollable MIPs with a wide selection of targets. This approach eliminates the need to decorate photochromic monomers with functional groups that are capable of binding with the template. Instead, well-established MIP recipes with common functional monomers can be used, adding a polymerizable photoswitchable molecule in a proper amount.

This work revealed the significance of the optimal amount of the spiropyran monomer to achieve photoactivatable molecularly imprinted binding sites. Fluorescence microscopy imaging and spectroscopic characterization supported the photoswitching characteristics owing to the anchored spiropyran units. A detailed characterization of the binding isotherm with the aid of the Freundlich model corroborated both the successful imprinting and the photomodulation of the binding sites. Cross-selectivity tests on analogous compounds and a structurally different one further confirmed molecular imprinting. With the selection of optimal binding conditions a complete release of the template could be achieved upon UV irradiation, albeit with a lower binding specificity. Repeated photoswitching cycles currently suggest that further improvements are necessary in order to increase long-term stability. We expect that the novel photocontrollable MIPs developed on the basis of this attractive approach may find applications in diverse areas as light-assisted solid phase extraction, ligand binding assays and photoresponsive renewable sensor elements.

ASSOCIATED CONTENT

Ⓢ Supporting Information

Additional information and movie file as noted in text. This material is available free of charge via the Internet at http://pubs.acs.org.

AUTHOR INFORMATION

Corresponding Author

*E-mail: Eric.Bakker@unige.ch.

Notes

The authors declare no competing financial interest.

ACKNOWLEDGMENTS

REFERENCES

(1) Fischer, E.; Hirshberg, Y. J. Chem. Soc. 1952, 4522−4524.

(2) Minkin, V. I. Chem. Rev. 2004, 104, 2751−2776.

(3) Chibisov, A. K.; Gorner, H. J. Phys. Chem. A 1997, 101, 4305−4312.

(4) Gorner, H. Phys. Chem. Chem. Phys. 2001, 3, 416−423.

(5) Ercole, F.; Davis, T. P.; Evans, R. A. Polym. Chem. 2010, 1, 37−54.

(6) Natali, M.; Giordani, S. Chem. Soc. Rev. 2012, 41, 4010−4029.

(7) Florea, L.; Diamond, D.; Benito-Lopez, F. Macromol. Mater. Eng. 2012, 297, 1148−1159.

(8) Fries, K. H.; Driskell, J. D.; Samanta, S.; Locklin, J. Anal. Chem. 2010, 82, 3306−3314.

(9) Gorner, H.; Chibisov, A. K. J. Chem. Soc., Faraday Trans. 1998, 94, 2557−2564.

(10) Evans, L.; Collins, G. E.; Shaffer, R. E.; Michelet, V.; Winkler, J. D. Anal. Chem. 1999, 71, 5322−5327.

(11) Byrne, R. J.; Stitzel, S. E.; Diamond, D. J. Mater. Chem. 2006, 16, 1332−1337.

(12) Scarmagnani, S.; Walsh, Z.; Slater, C.; Alhashimy, N.; Paull, B.; Macka, M.; Diamond, D. J. Mater. Chem. 2008, 18, 5063−5071.

(13) Ipe, B. I.; Mahima, S.; Thomas, K. G. J. Am. Chem. Soc. 2003, 125, 7174−7175.

(14) Andersson, J.; Li, S.; Lincoln, P.; Andreasson, J. J. Am. Chem. Soc. 2008, 130, 11836−11837.

(15) Radu, A.; Byrne, R.; Alhashimy, N.; Fusaro, M.; Scarmagnani, S.; Diamond, D. J. Photoch. Photob. A 2009, 206, 109−115.

(16) Mistlberger, G.; Crespo, G. A.; Xie, X.; Bakker, E. Chem. Commun. 2012, 48, 5662−5664.

(17) Xie, X.; Mistlberger, G.; Bakker, E. J. Am. Chem. Soc. 2012, 134, 16929−16932.

(18) Mistlberger, G.; Xie, X.; Pawlak, M.; Crespo, G. A.; Bakker, E. Anal. Chem. 2013, 85, 2983−2990.

(19) Arai, K.; Shitara, Y.; Ohyama, T. J. Mater. Chem. 1996, 6 (11), 11−14.

(20) Tork, A.; Boudreault, F.; Roberge, M.; Ritcey, A. M.; Lessard, R. A.; Galstian, T. V. Appl. Opt. 2001, 40, 1180−1186.

(21) Rosario, R.; Gust, D.; Hayes, M.; Jahnke, F.; Springer, J.; Garcia, A. A. Langmuir 2002, 18, 8062−8069.

(22) Radu, A.; Scarmagnani, S.; Byrne, R.; Slater, C.; Lau, K. T.; Diamond, D. J. Phys. D: Appl. Phys 2007, 40, 7238−7244.

(23) Sellergren, B., Ed. Molecularly Imprinted Polymers: Man-Made Mimics of Antibodies and Their Applications in Analytical Chemistry; Elsevier: Amsterdam, 2001.

(24) Marxtibbon, S.; Willner, I. J. Chem. Soc.−Chem. Commun. 1994, 10, 1261−1262.

(25) Minoura, N.; Idei, K.; Rachkov, A.; Choi, Y. W.; Ogiso, M.; Matsuda, K. Macromolecules 2004, 37, 9571−9576.

(26) Gong, C.; Lam, M. H.-W.; Yu, H. Adv. Funct. Mater. 2006, 16, 1759−1767.

(27) Gomy, C.; Schmitzer, A. R. Org. Lett. 2007, 9, 3865−3868.

(28) Takeuchi, T.; Akeda, K.; Murakami, S.; Shinmori, H.; Inoue, S.; Lee, W.-S.; Hishiya, T. Org. Biomol. Chem. 2007, 5, 2368−2374.

(29) Gong, C.; Wong, K.-L.; Lam, M. H. W. Chem. Mater. 2008, 20, 1353−1358.

(30) Fang, L.; Chen, S.; Zhang, Y.; Zhang, H. J. Mater. Chem. 2011, 21, 2320−2329.

(31) Fang, L.; Chen, S.; Guo, X.; Zhang, Y.; Zhang, H. Langmuir 2012, 28, 9767−9777.

(32) Ma, Y.; Zhang, Y.; Zhao, M.; Guo, X. Z.; Zhang, H. Q. Chem. Commun. 2012, 48, 6217−6219.

(33) Ma, Y.; Zhang, Y.; Zhao, M.; Guo, X.; Zhang, H. Mol. Imprint. 2012, 1, 3−16.

(34) Ferrer, I.; Lanza, F.; Tolokan, A.; Horvath, V.; Sellergren, B.; Horvai, G.; Barcelo, D. Anal. Chem. 2000, 72, 3934−3941.

(35) Turiel, E.; Martin-Esteban, A.; Fernandez, P.; Perez-Conde, C.; Camara, C. Anal. Chem. 2001, 73, 5133−5141.

(36) Pap, T.; Horvath, V.; Tolokan, A.; Horvai, G.; Sellergren, B. J. Chromatogr., A 2002, 973, 1−12.

(37) Friedle, S.; Thomas, S. W., III Angew. Chem., Int. Ed. 2010, 49, 7968−7971.

(38) Wang, J. F.; Cormack, P. A. G.; Sherrington, D. C.; Khoshdel, E. Angew. Chem., Int. Ed. 2003, 42, 5336−5338.

(39) Wang, J. F.; Cormack, P. A. G.; Sherrington, D. C.; Khoshdel, E. *Pure Appl. Chem.* **2007**, *79*, 1505−1519.

(40) Horvath, V.; Lorantfy, B.; Toth, B.; Bognar, J.; Laszlo, K.; Horvai, G. *J. Sep. Sci.* **2009**, *32*, 3347−3358.

(41) Shiraishi, Y.; Itoh, M.; Hirai, T. *Phys. Chem. Chem. Phys.* **2010**, *12*, 13737−13745.

(42) Matsui, J.; Miyoshi, Y.; Doblhoffdier, O.; Takeuchi, T. *Anal. Chem.* **1995**, *67*, 4404−4408.

(43) Andersson, L. I. *Anal. Chem.* **1996**, *68*, 111−117.

(44) Toth, B.; Pap, T.; Horvath, V.; Horvai, G. *Anal. Chim. Acta* **2007**, *591*, 17−21.

(45) Ye, L.; Weiss, R.; Mosbach, K. *Macromolecules* **2000**, *33*, 8239−8245.

(46) Toth, B.; Pap, T.; Horvath, V.; Horvai, G. *J. Chromatogr., A* **2006**, *1119*, 29−33.

(47) Rampey, A. M.; Umpleby, R. J.; Rushton, G. T.; Iseman, J. C.; Shah, R. N.; Shimizu, K. D. *Anal. Chem.* **2004**, *76*, 1123−1133.